University of Huddersfield Repository

Arebi, Lufti, Gu, Fengshou and Ball, Andrew

A comparative study of misalignment detection using a novel Wireless Sensor with conventional Wired Sensors

Original Citation

A comparative study of misalignment detection using a novel Wireless Sensor with conventional Wired Sensors

L Arebi, F Gu and A Ball
University of Huddersfield, Queensgate, Huddersfield HD1 3DH, UK

Email address: l.arebi@hud.ac.uk; f.gu@hud.ac.uk and andrew.ball@hud.ac.uk

Abstract. The advancement in low cost and low power MEMS sensors makes it possible to develop a cost-effective wireless accelerometer for condition monitoring. Especially, the MEMS accelerometer can be mounted directly on a rotating shaft, which has the potential to capture the dynamics of the shaft more accurately and hence to achieve high monitoring performance. In this paper a systematic comparison of shaft misalignment detection is conducted, based on a bearing test rig, between the wireless sensor measurement scheme and other three common sensors: a laser vibrometer, an accelerometer and a shaft encoder. These four sensors are used to measure simultaneously the dynamic responses: Instantaneous Angular Speed (IAS) from the encoder, bearing house acceleration from the accelerometer, shaft displacements from the laser vibrometer and angular acceleration from the wireless sensor. These responses are then compared in both the time and frequency domains in detecting and diagnosing different levels of shaft misalignment. Results show the effectiveness of wireless accelerometer in detecting the faults.

Keywords: *Wireless Accelerometer, Misalignment, Vibration, Encoder, Instantaneous Angular Speed.*

1. Introduction

Shaft misalignments cause not only machine vibration but also additional dynamic load which accelerates machine deterioration. In industry, 30% of a machine's downtime is due to the poorly aligned machines [1]. Misalignment is estimated to cause over 70% of rotating machinery's vibration problems [2]. There has been much research on experimental and analytic study of misalignments considering vibration and dynamic forces, which showed that the vibration, measured at bearing houses, due to coupling misalignment mainly occur at the even multiples of the rotor speed [4-12].

However, a misaligned rotor generates very complicated dynamic responses due to uncertainties of rotor constructions including bearing stiffness, coupling types, manufacturing and installation accuracy, mounting base dynamics, lubrication performance, thermal deformations etc. Many different models [4-8] have been developed to include these influences in different ways. Although these models produce a good prediction in particular cases, they are not so generic as to include all the factors. This means that the accurate dynamics of a shaft needs to be determined through experimental studies.

The most common way to measure the dynamics for diagnosing shaft related problems is to place an accelerometer on a bearing house. Obviously, because of the attenuation and distortion due to bearing structure dynamics, it is difficult to obtain the true dynamic behavior of the shaft.

To avoid the influences of the sensor position, it is sensible to place a sensor on the shaft directly. Thanks to the advancement in low cost and low power MEMS sensors, it is possible to develop a cost-effective measurement scheme by placing a wireless accelerometer on the rotating shaft for monitoring the dynamics of the shaft and achieve a more accurate fault diagnosis [13] in a remote way.

To confirm the performance of the wireless measurement scheme in monitoring shaft dynamics, this paper focuses on a comparative study of monitoring shaft misalignments using a wireless accelerometer mounted directly on a shaft and three other sensors: laser vibrometer, accelerometer and shaft encoder.

2. Test facility and method

A bearing test rig, shown in figure 1, was employed in this experimental study. It consists of a 3-phase electrical induction motor to provide a prime power source and a DC generator to apply load to the motor. The motor is connected to the generator through two shafts, which are connected by three pairs of flexible couplings and supported by bearings in two bearing housings. The construction allows the study of different types of misalignments such as angular and parallel misalignments in different parts of the shaft system. The wireless accelerometer was mounted directly on the shaft connecting to the shaft of the motor while an encoder was mounted at the rotor end of the induction motor as shown in figure 1 and 2. The test rig can run in a speed range from 60rpm to 1420rpm.
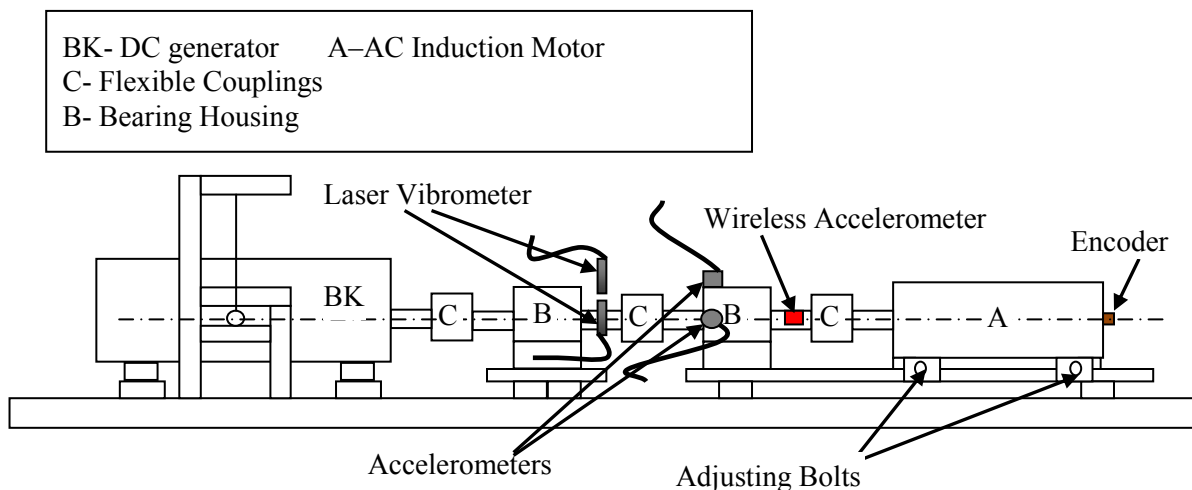

Figure 1. Test rig schematic and wireless sensor placement.

2.1. Encoder

An incremental shaft encoder type RI32, shown in figure 2, is used in this experiment which is usually used to measure the Instantaneous Angular speed (IAS) [14]. This device provides two outputs: 100 electrical pulse trains per revolution and one pulse per revolution. It is the 100 pulse train that provides rotational oscillation of the shaft and used to benchmark the output from the wireless sensor [15].

Figure 2. Incremental Shaft Encoder Type RI32 [15].

2.2. Laser vibrometer

The principle of a laser vibrometer shown in figure 3 (optoNCDT1300 from Micro-Epsilon) is optical triangulation where a light spot is projected onto the target surface. This depends on the distance; the diffused fraction of the reflection of this light is focussed onto the sensitive element by receiving lens with respect to the optical axis of the laser beam. The controller measures any displacement change within the surface. The resolution of the sensor is 4μm (static) and 10μm (dynamic) (Micro-Epsilon).

Figure 3. optoNCDT1300 (Micro-Epsilon) [16].

Figure 4. Accelerometer images.

2.3. Accelerometer

The accelerometers are piezoelectric based YD-185TNC series accelerometers, which both have a flat frequency response in the range 0.5Hz to 5000 Hz. In addition, the sensitivity of the vertical positioned sensor (SN00016) is 5.106 mV/ms^{-2} and the horizontal positioned sensor (SN00039) is 4.960 mV/ms^{-2}., both operating under 12-24 VDC, as shown in figure 4.

A MEMS accelerometer wireless sensor, developed by [17], is mounted directly on the second shaft connecting to the shaft of the motor in figure 5. The principal sensitivity axis of the sensor is along the tangential direction of shaft rotation as depicted in the left drawing of figure 5. To benchmark the results from the wireless sensor, a shaft encoder is mounted at the end of the induction motor. In addition, two accelerometers are connected to the bearing housing close to the motor as shown in figure 1; one is on the vertical position while the second one is on the horizontal position of the bearing housing. Also, two laser vibrometers are installed to monitor the shaft vibration in both vertical and horizontal directions of the shaft as shown in figure 1. All sensors channels are measured simultaneously through data acquisition (YE7600) with 16 channels at a sampling rate of 96 kHz. At such a high rate, the signals from the sensors can be recorded accurately.
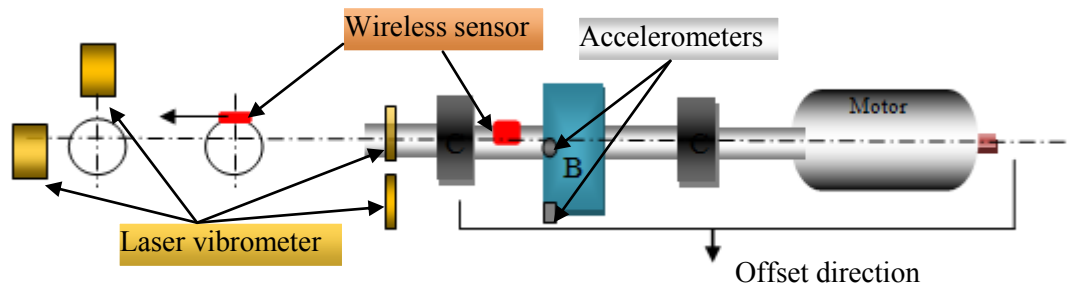

Figure 5. Schematic diagram of misaligned shaft.

During post-processing, the Duty cycle signal (DCS) from the wireless sensor is low pass filtered (500Hz) to obtain the acceleration signal at tangential direction. The pulse train signal is applied by an FFT based demodulation algorithm [18] to obtain an IAS signal. As only a relative comparison of detection performance is made between the wireless sensor and the shaft encoder, the unit of angular speed is used directly, rather than converting it into angular acceleration by multiplying IAS by a constant of angular frequency. The acceleration waveforms from the accelerometers are directly compared, while the displacement from the laser vibrometer is a relative comparison of detection performance with other sensors.

2.4. Test procedure

The test rig was operated under a fixed load of 50% of the rated load but at different speeds: 284, 426, 568, 710, 852, 994, 1136, 1278 and 1420 rpm to examine the frequency response and sensitivity of the wireless sensor. Different shafts of the rig are tuned with minimal misalignment which was confirmed through a static measurement of a dial meter and dynamic measurements of all the sensors. The data was then collected from all sensors simultaneously as the baseline reference.

Using the dial meter, the first level of misalignment between shafts was set as 0.3mm in a horizontal direction at which repeatable results could be obtained for all sensors. The test rig then ran under the operating conditions for data collection at this misalignment level. This step was repeated for other higher misalignment levels: 0.4mm and 0.5mm.

The collected datasets were then processed using a Matlab program to perform comparisons of time waveforms and frequency spectra.

3. Results and discussion

3.1. Waveform Variation

Figure 6 shows typical waveforms from a wireless sensor for 0.3mm misalignment level and shaft speeds (284-1420rpm). As illustrated by the top row of figure 6, the outputs of the wireless sensor for a baseline case show clear periodic oscillations respective to shaft fundamental period. This may be due to inevitable misalignment from other shafts in the system. In contrast, cases with higher degrees of misalignments exhibit a small increase in waveform amplitudes. In addition, the waveform shape also shows considerable change for higher misalignment level at high speed. These give good indications for detecting and diagnosing the occurrence of misalignments.
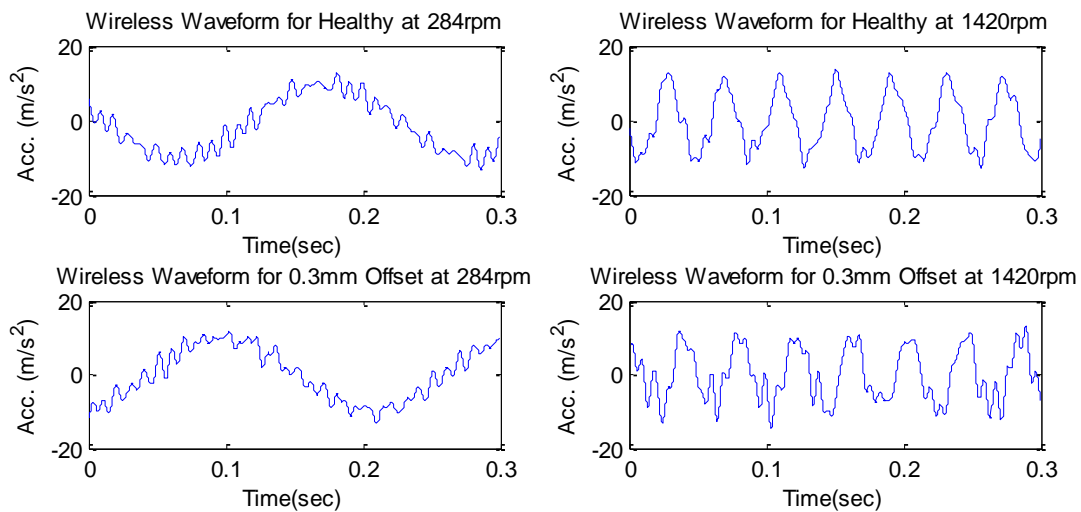

Figure 6. Waveforms from wireless sensor for different shaft conditions at higher and lower speeds.

IAS waveforms from the encoder in figure 7 show similar periodic oscillation with that of the wireless sensor. With higher degrees of misalignments it exhibits slight decreases in waveform amplitudes at low speed. However, an increase in waveform amplitudes has been observed at high speed
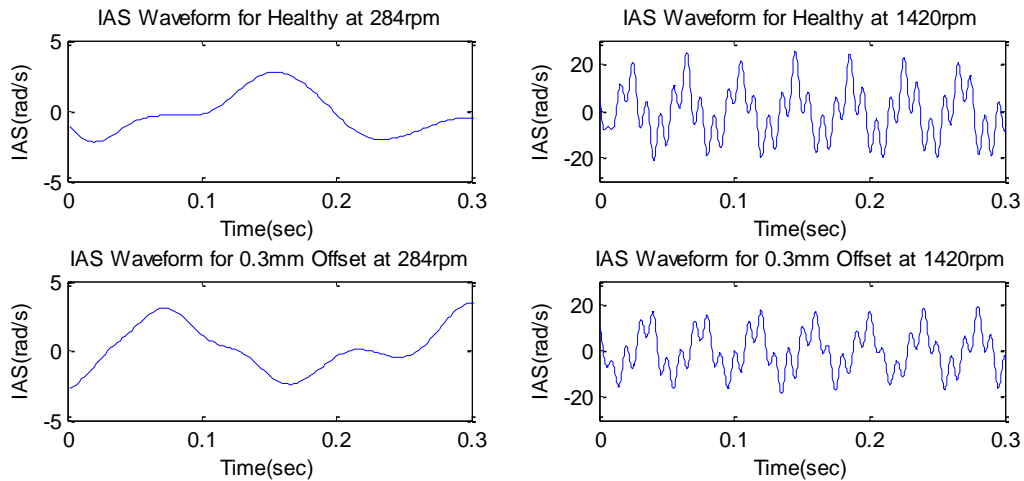

Figure 7. IAS waveforms from encoder for different shaft conditions at higher and lower speeds.

Figure 8 illustrates the outputs of the accelerometer sensors in vertical and horizontal directions. The waveforms have been badly contaminated by high frequency noise, making the periodic feature hardly able to be observed. The waveform amplitudes exhibit small change with different degrees of misalignment at low speed whereas significant increase at high speed. In addition, the horizontal vibration waveform amplitudes are slightly higher than that of the vertical one, and increase with misalignment levels as shown in figure 8.
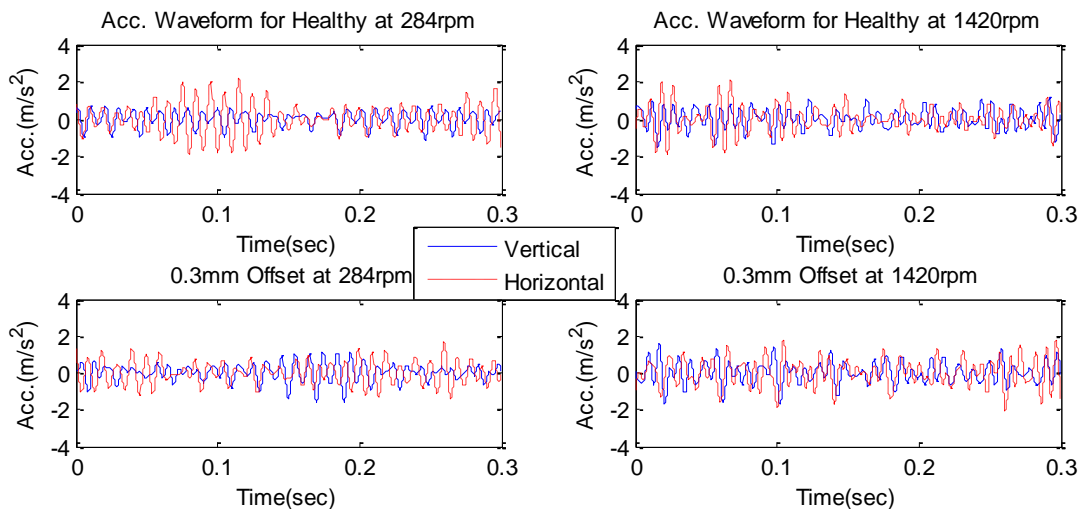

Figure 8. Waveforms from Accelerometer for different shaft conditions at higher and lower speeds.

The displacement waveforms from the laser sensor are illustrated in figure 9. The waveforms show clear periodicity with respect to the shaft rotation. However, its amplitude exhibits a very small increase with misalignment levels at low speed, whereas at high speed the amplitude decreases with

misalignment levels. Comparing between waveforms at the two different directions has found that the horizontal one is lower than that of the vertical one, which is somehow inconsistent with the misalignment induced to the system.
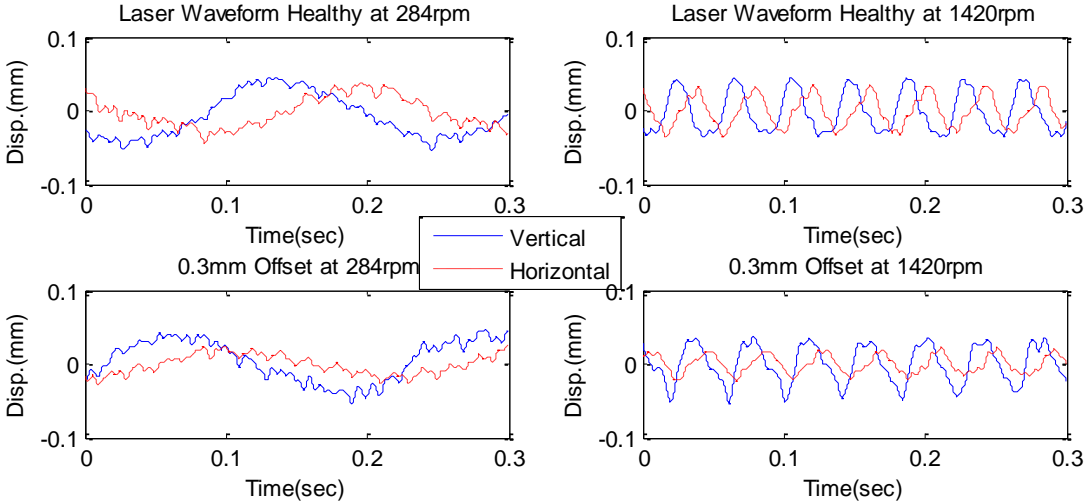

Figure 9. Waveforms from Laser vibrometers for different shaft conditions at higher and lower speeds.

From the above waveform based analysis, the wireless sensor and accelerometers are more likely to detect the misalignment than the other sensors.

3.2. Spectrum Variation

To gain a better understanding of the measured responses for identifying accurate features to differentiate the misalignment, Fast Fourier Transform (FFT) is applied to all signals to obtain corresponding spectra, shown in figures 10, 11, 12 and 13 respective to wireless sensor, IAS, accelerometer and laser vibrometers.

Figure 10 shows the wireless sensor spectra. The high amplitude of 1X running speed is mainly due to the gravity effect of its rotation around the shaft in all conditions. The faint higher harmonics are representing inevitable rotor imbalance or misalignment in the baseline spectra. Comparing the spectra between the baseline and the misaligned case, it was found that the amplitude of 2X running speed has little change at low speed whereas a significant increase is seen at the high speed due to effect of the imbalance caused by misalignment. However, amplitudes of the harmonics higher than 2X only show marginal increase at high speed, showing less effect of misalignment on high frequency vibration. Nevertheless, the considerable amplitude increase at 2X is an indication for misalignment.

The encoder spectra in figure 11 illustrate a small increase in the amplitude of 1X running speed with an increase in rotor speed in the baseline spectra. With the misalignment level induced, the amplitude exhibits a decrease compared to the baseline. On the other hand, the amplitude of 2X running speed is increased by high speed and high level of misalignment. The small change in spectral amplitude of 2X is due to the position of the encoder at the far end of the shaft.

Figure 12 presents the accelerometer spectra at low and high speed. The amplitude of 1X running speed in the vertical direction is faintly increased with increase of speed, whereas the horizontal one is increased significantly. With the misalignment case, the horizontal 1X amplitude increases more than that of vertical one. The 2X component amplitudes exhibit a small increase with different levels of misalignment at low speed, whereas significant increase at high speed. In addition, the horizontal 2X amplitudes are slightly higher than that of the vertical one, and increase with misalignment levels as illustrated in figure 12.

The laser vibrometer spectra in figure 13 show that 1X amplitude decreases for both vertical and horizontal ones with the increase of both speed and misalignment level. Comparison between 2X amplitude at the two different directions has found that the horizontal one is lower than that of the vertical one, which is somehow inconsistent with the misalignment levels induced to the system as shown in figure 13.

From the above discussion, it is clear that the 2X amplitude increases with the increase of both speed and misalignment level. However, the wireless sensor produces more significant increase than that of other sensors.
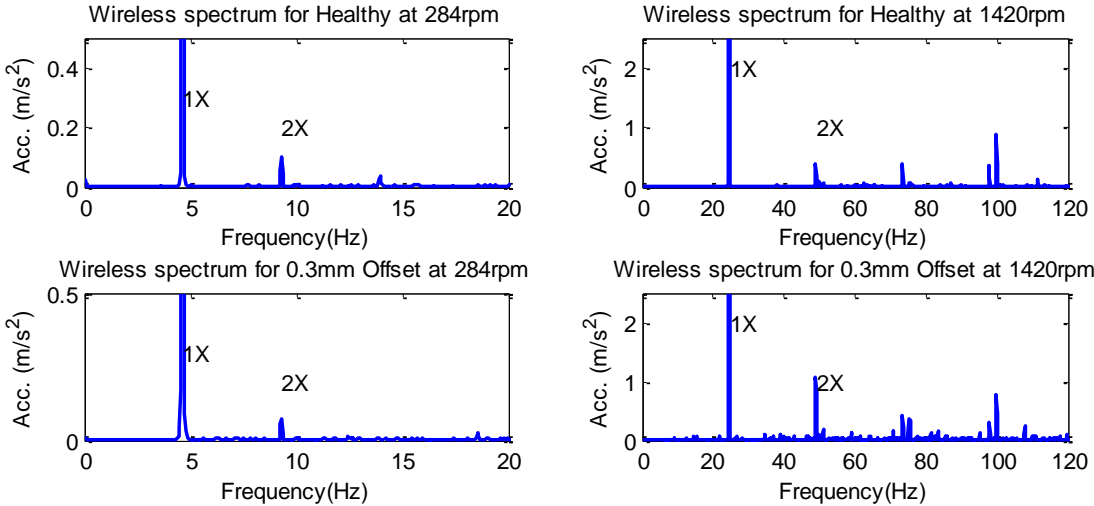

Figure 10. Spectra from wireless sensor under different conditions.
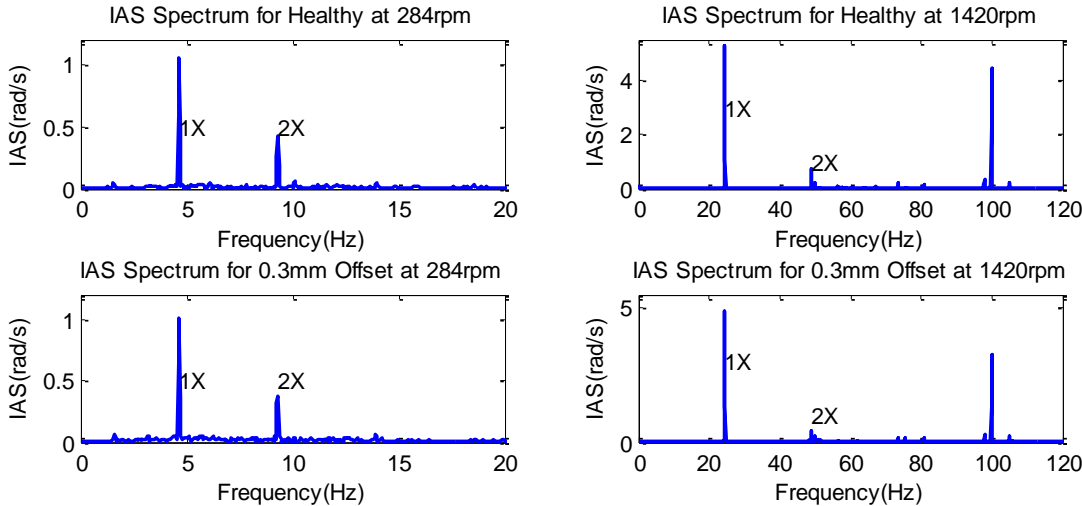

Figure 11. Spectra from Encoder (IAS) under different conditions.

3.3. Detection and Diagnosis Performance

To give a more accurate result for misaligment diagnosis and comparison between sensors, the amplitude at 1X and 2X runing speed are extracted from their spectra and presented with respect to speed variations in figure 14 and 15 respectively.

Comparing the trends between different sensors and misalignment levels, it was found in figure 14 that 1X compnent for wireless sensor, encoder and laser vibrometer is not able to separate baseline and misaligned cases. However, the accelerometer in vertical and horizontal shows a clear discrepancy between baseline and different misalignment levels. The horizontal accelerometer shows better separation between baseline and misalignment levels at high speed increases, but different levels of misalignments are not consistent. This argument proves that the misalignment cannot be clearly found based on the amplitude of 1X runing speed for all the sensors.
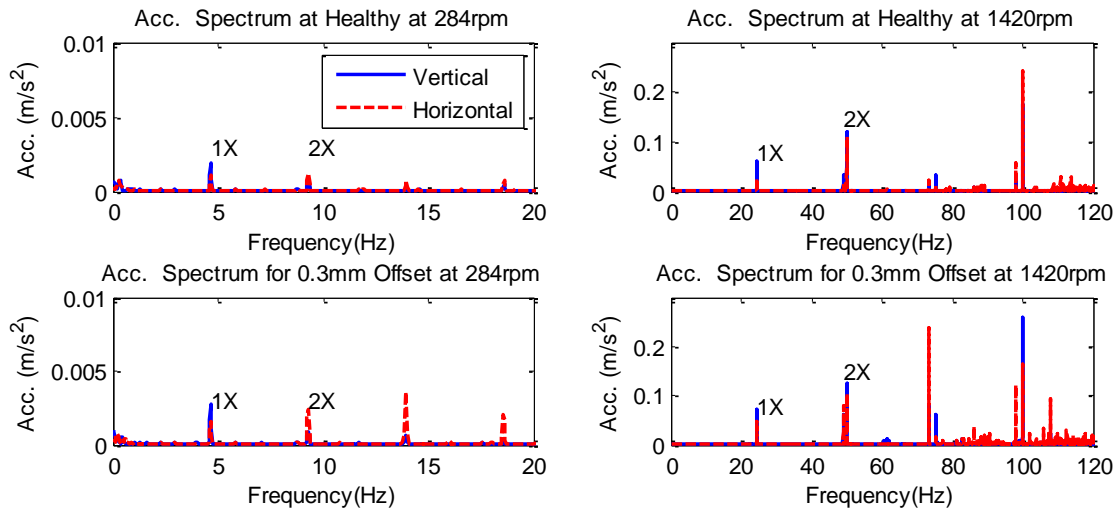

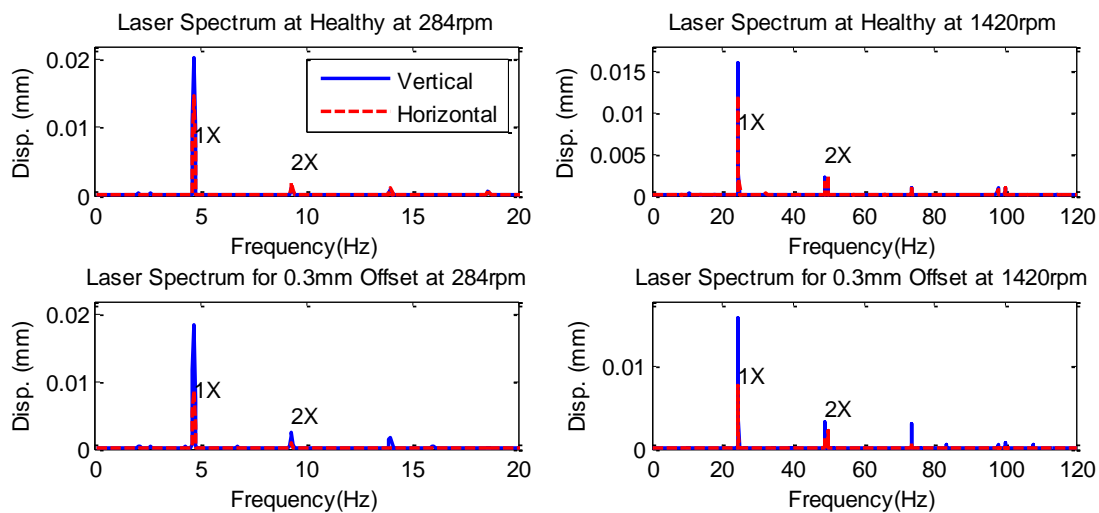**Figure 12.** Spectra from Accelerometer under different conditions.

Figure 13. Spectra from Laser vibrometer under different conditions.

On the other hand, the amplitude 2X component in figure 15 shows that several sensors such as wireless sensor, accelerometers and encoder could be used for misalignment diagnosis as there are certain amplitude differences between misalignment cases and speed. However, the most extraordinary one is the wireless sensor that is able to produce not only correct difference from the baseline, but also full separation between different levels of misalignments for all speeds. Moreover, these results agree with the wireless sensor model results proven by [19] and with results reported by other researchers [4-8].
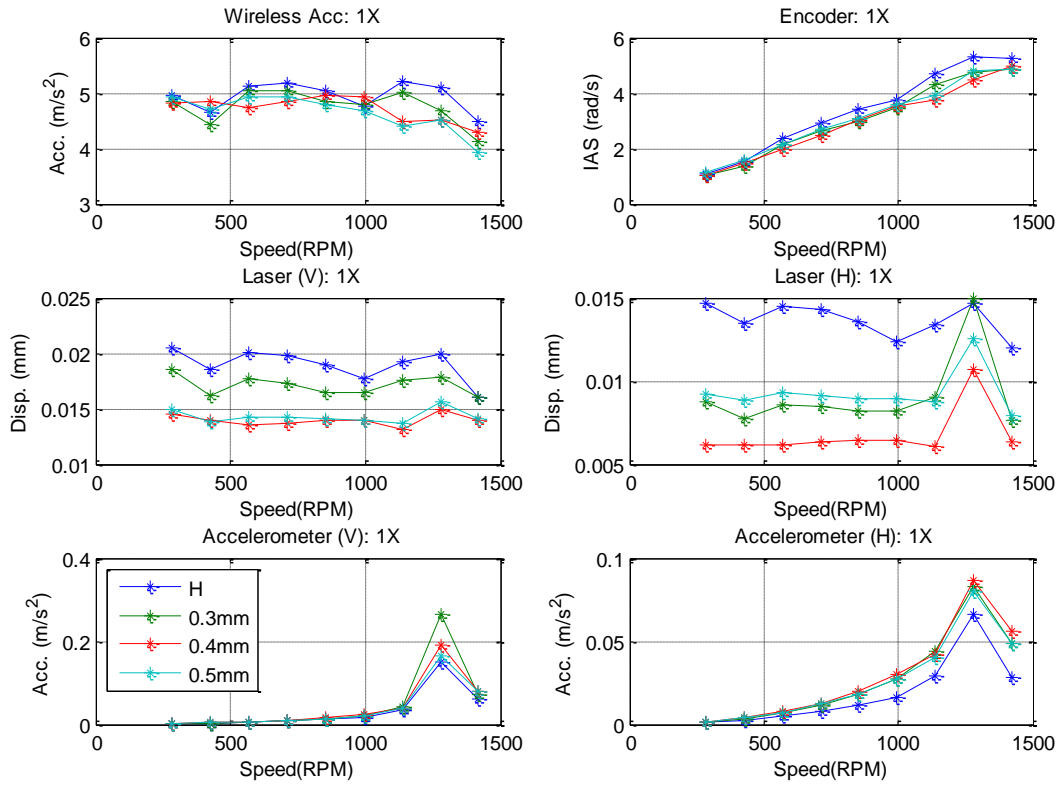
Figure 14. Spectral amplitudes at 1X running speed versus speed and misalignments.
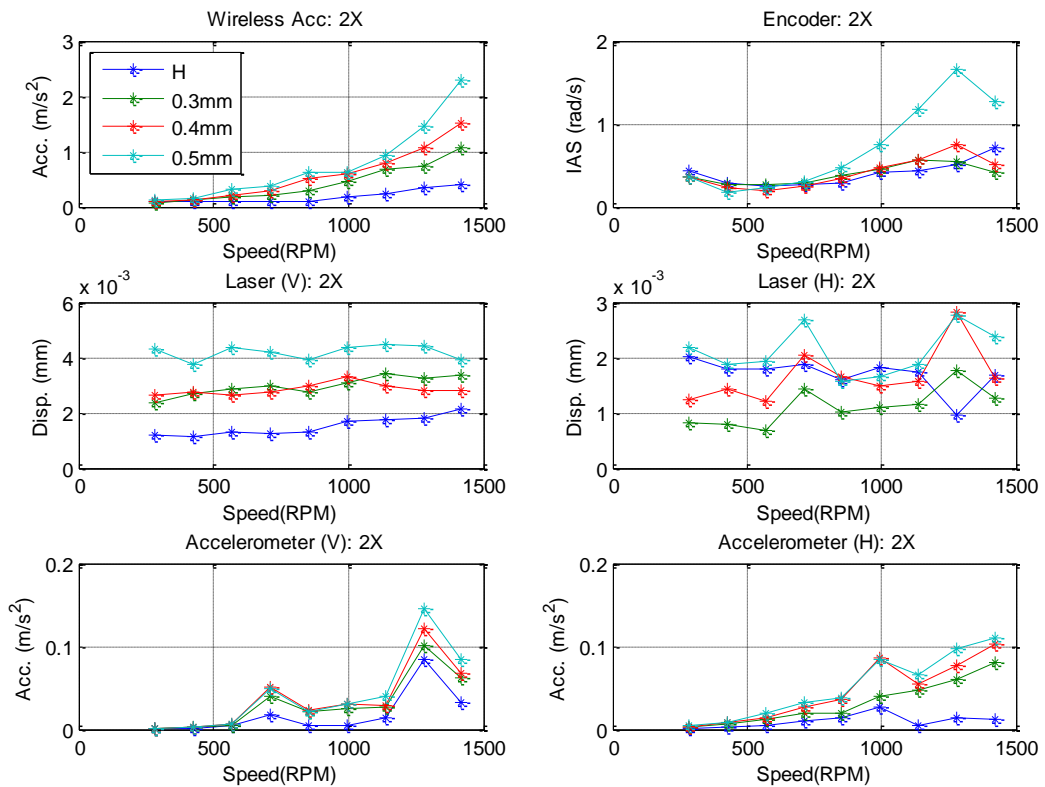

Figure 15. Spectral amplitudes at 2X running speed versus speed and misalignments.

4. Conclusions

The comparison of vibrations from different sensors has shown a slight change in the amplitude of the signals for different misalignment levels. The amplitude increases with speed largely, but its overall level could not show a consistent trend with the successive changes of misalignments because of high frequency noises from other vibrations.

The spectral analysis shows at amplitude 1X running speed component that all sensors failed to differentiate different levels of misalignment. However, the amplitude 2X running speed allows the misalignments to be separated with different degrees of success depending on the sensors used:

- The wireless sensor produces full separation of different misalignment levels and shows a unique increasing trend with speeds.
- IAS allows the separation of the high misalignment levels.
- Vertical displacement from the vibrometer shows misalignment separation from the baseline but is not very consistent with misalignment levels.
- Horizontal acceleration shows a very similar performance as that of the wireless sensor, but its trend has oscillations with speeds.

5. References

[1] Hariharan V, Srinivasan P and Kongu E 2009 Vibration analysis of misaligned shaft –ball bearing system. *Indian J. of Sci. and Technol.*, **2** (**9)**, ISSN: 0974- 6846

[2] Bognatz S R 1995 Alignment of critical and non critical machines. *Orbit* 23–25

[3] Tejas H, AshishK D 2009 Experimental investigations on vibration response of misaligned rotors. *Mechanical Systems and Signal Processing*, **23(7)**, 2236–52

[4] Vance JM 1988 *Rotor dynamics of Turbomachinery* (New York: John Wiley & Sons)

[5] Goodman MJ 1989 *Dynamics of rotor – bearing systems* (London: Unwin Hyman Ltd)

[6] Gibbons C B 1976 *Coupling misalignment forces*. Proceedings of the 5th Turbo Machinery Symposium, Gas Turbine Laboratory, Texas A & M University, 111–116

[7] Xu M, Marangoni RD 1994a Vibration analysis of a motor-flexible coupling-rotor system subjected to misalignment and unbalance Part I: Theoretical model and analysis. *Journal of Sound and Vibration*, **176(5)**, 663–679.

[8] Sekhar A S, Prabhu B S 1995 Effects of coupling misalignment on vibration of rotating machines. *Journal of Sound and Vibration* **185**, 655–671.

[9] Dewell DL and Mitchell LD 1984 Detection of a misaligned disk coupling using spectrum analysis. ASME Trans. *J. Vibration, Acoustics, Stress & Reliability Design*. **106**, 9-16

[10] Piotrowski J 1995 *Shaft Alignment Handbook* (New York: Marcel Dekker Inc.)

[11] Stephen J, Wesley J H and Andrew E 1999 Motor Shaft Misalignment Bearing Load Analysis. Maintenance and Reliability Center College of Engineering, The University of Tennessee, Computational Systems Incorporated

[12] Lees A W 2007 Misalignment in rigidly coupled rotor. *J. of Sound and Vibration* **305,**261–271

[13] Arebi L, Yibo F, Fengshou Gu and Ball A 2010 Investigation of Wireless Sensor   Directly Deployed on Rotating Shaft and Its Potential for Machinery Condition Monitoring. *Proc.* Of COMADEM2010, (Japan).

[14] Li Y, Gu F, Ball A and Bennett N 2004 The measurement of Instantaneous Angular Speed. *Mechanical Systems and Signal Processing*, **19(4)**, 786-805.

[15] Hengstler, Inc. TECHNICAL DATASHEET Incremental Encoder RI32 http://www.hengstler.com/en/products/shop.php,catID=1011&artID=34 [1/2/2009].

[16] Micro-Epsilon website http://www.micro-epsilon.de/download/products/cat--optoNCDT--en.pdf

[17] Arebi L, Fengshou Gu and Ball A 2010 Rotor Misalignment Detection using a   Wireless Sensor and a Shaft Encoder. *Diagnostic Engineering Research Centre*. University of Huddersfield UK. CEARC2010 *conf.*

[18] Gu F, Yesilyurt I, et al 2006 An Investigation of the Effects of Measurement Noise in the Use

of Instantaneous Angular Speed for Machine Diagnosis, *Mech. Sys. and Signal Proc.*, **20(6)** , pp.1444-60.

[19]   Arebi L, Fengshou Gu and Ball A 2011 Misalignment Detection using a Wireless Sensor Mounted on a Rotating Shaft. *Proc. of the 24th Int. Cong. on Condition Monitoring and Diagnostics Engineering Management* (COMADEM2011), PP.1289- 99.